PERGAMON

International Journal of Heat and Mass Transfer 44 (2001) 4679–4691

International Journal of HEAT and MASS TRANSFER

www.elsevier.com/locate/ijhmt

Simulation by solutal convection of a thermal plume in a confined stratified environment: application to displacement ventilation

O. Auban [a], F. Lemoine [b,*], P. Vallette [b], J.R. Fontaine [a]

[a] *Département Ingéniérie des Procédés, Institut National de Recherche et Sécurité, Avenue de Bourgogne, BP 27, F-54501 Vandoeuvre-lès-Nancy Cedex, France*

[b] *LEMTA, C.N.R.S. UMR 7563, 2 avenue de la Forêt de Haye, BP 160, F-54504 Vandoeuvre-lès-Nancy Cedex, France*

Received 20 October 2000; received in revised form 23 February 2001

Abstract

This paper describes the experimental study, by solutal simulation, of a thermal plume in a confined stratified environment, a situation encountered in displacement ventilation systems. The criteria enabling similarity to be established between the thermal plume in air and the solutal plume in a hydraulic model are discussed. Density stratification is detected by a planar laser-induced fluorescence (PLIF) technique. Criteria for defining the interface height and thickness are determined After validation of these criteria in the fully developed region of the plume in a confined stratified environment, a formulation of the stratification height in the region close to the source has been established.

Keywords: Solutal simulation; Displacement ventilation; Plume; Planar laser-induced fluorescence (PLIF); Density stratification

1. Introduction

Theoretical and experimental studies of plumes in confined stratified environment have numerous applications, especially in the field of ventilation of rooms, and more specifically in the area of displacement ventilation. This ventilation principle is based on the presence of heat sources in the room's area of occupation. Each of these sources generates a natural convection thermal plume which entrains an ambient air flow Q which becomes increasingly large as it rises. A fresh air volume flow Q_1 is supplied in the lower section of the room and this same flow is exhausted in the upper section. If Q_1 is less than the flow rate Q entrained by the plume at the ceiling level, a vertical temperature stratification is established in the room. Ventilation of the room at a given flow rate is designed to maintain the height of this stratification constant. The flow, in steady-state regime, thus shows two main regions relatively uniform in temperature: a lower region supplied with fresh air in which the plumes develop, and a hotter region of recirculated air (Fig. 1). The stratification height should correspond to the level for which the flow rate entrained by the plumes is equivalent to the fresh air flow rate, also called ventilation flow rate. At this stratification height, real situations show no sharp temperature discontinuity: the two flow regions are separated merely by an interface region in which the temperature varies sharply with the height. In the lower region, it seems that the plume develops in a manner completely similar to what is observed in a uniform infinite environment. In the upper region, the central flow is renewed by recirculation and the density is constant. In this region, the flow is no longer characterised by its buoyancy flux but by its momentum flux, as in the case of a jet [1]. The turbulent plume flows coming from buoyancy sources have been studied extensively for a great many years [2]. Experimentally, the flows studied were either convection

* Corresponding author. Tel.: +33-03-83-99-57-32; fax: +-03-83-99-99-44.

E-mail address: flemoine@enserm.inpl-nancy.fr (F. Lemoine).

0017-9310/01/$ - see front matter
PII: S0017-9310(01)00117-X

Nomenclature

B_s	buoyancy flux, $B_s = g\frac{\Delta\rho}{\rho_0}Q_s$ (m^4 s^{-3})
C	molecular concentration of the fluorescent dye (mol m^{-3})
C_s	tracer concentration at source
D_t	thermal diffusivity (m^2 s^{-1})
a	molecular diffusion coefficient of ethanol in water (m^2 s^{-1})
D	thermal source diameter (m)
D_s	source diameter in the model (m)
F	concentration fluctuations flatness factor
g	gravitational acceleration (m s^{-2})
k	thermal conductivity (W m^{-1} K^{-1})
L_m	lateral size of an elementary mesh (m)
Nu	Nusselt number
Pr	Prandtl number
Q	plume flow rate (m^3 s^{-1})
Q_1	ventilation flow rate (m^3 s^{-1})
Q_s	source flow rate (m^3 s^{-1})
R_m	mesh size (m), $R_m = \sqrt{2}/2L_m$
Ra	Rayleigh number
Ra_m	solutal Rayleigh number
S	concentration fluctuations skewness factor
Sc	Schmidt number
Sh	Sherwood number
T	absolute temperature (K)
w	vertical velocity component (m s^{-1})
z	elevation above source (m)
z_c	ceiling elevation (m)
z_i	interface position (m)
z_v	virtual origin position (m)

Greek symbols

α	entrainment constant
β_m	mass expansion coefficient (m^3 kg^{-1})
δ	interface thickness (m)
v	kinematic viscosity (m^2 s^{-1})
ρ	density of the fluid injected in the source (kg m^{-3})
ρ_0	water density (reference) (kg m^{-3})
σ	concentration fluctuations standard deviation

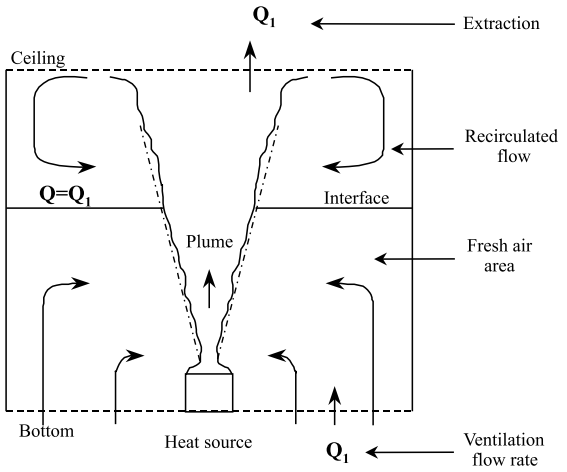

Fig. 1. Thermal plume in a confined and ventilated enclosure and principle of displacement ventilation.

thermal plumes [3] or buoyant jets for which an initial momentum is imparted to the source [4,5]. These plumes were studied mainly in a free configuration, in an environment of uniform density. Assuming a self-similar mean behaviour, it is then possible, based on a dimensional analysis [6], to describe the behaviour of a fully developed turbulent plume by correlations involving only two parameters. The first is the distance from the source, for which is substituted the distance relative to a virtual origin in the case of a non-localised source, and the second is the initial buoyancy flux B_s. Much work, both experimental [4] and theoretical [7], has confirmed this approach and refined the knowledge of flows of fully developed plumes, especially from the viewpoint of turbulence [4,5]. However, given the large number of possible source geometries, the study of flow in the region close to the source, for which fully developed plume correlations are not applicable, has remained a more difficult subject to deal with. Various experimental references are available to identify the virtual origin of simple geometry sources, such as the case of a plate, a vertical cylinder [8,9] or a spherical cap [10]. However, there are still relatively few formal approaches to characterise the vicinity of the source [11]. To approximate characteristic displacement ventilation configurations, but without making use of real conditions of similarity between flows, several authors have designed experiments concerning plumes in a ventilated enclosure on models or test units [12–14]. In all approaches to the phenomenon of stratification in an enclosure [15], no precise definition of the stratification height nor the interface thickness has been given. Some authors define this height based on the mean vertical temperature profiles in the enclosure [13]. Baines [16] studies the phenomenon by solutal convection and identifies the interface height through visualisation by the shadowgraph technique. These authors have shown that the stratification height measured rather far from the source was proportional to the quantity $B_s^{-1/5}Q_1^{-3/5}$ [12,16].

This paper describes a plume flow in a confined enclosure in which the ventilation conditions result in vertical stratification. The study is performed by solutal

similarity, endeavouring to reproduce industrial conditions. The buoyancy flux is created by injecting ethanol into water. The fluid contaminated by the buoyancy source is marked by a fluorescent tracer. Stratification is created by the intake of a flow of fluid not contaminated by the source and by exhausting this same flow via the ceiling. The field of concentration of the tracer representative of the field contaminated by the source is displayed by a planar laser-induced fluorescence (PLIF) technique. The velocity field is measured by laser Doppler velocimeter (LDV).

After validation of the experiment in an infinite environment relative to known results, the experimental results presented concern characterisation of the interface and enable definition of an interface elevation and thickness. The formulation of laws describing the stratification height as a function of various parameters is then presented and extended to the case, little discussed in the literature, in which this height is located in the region close to the source.

2. Principles of hydraulic solutal simulation

The principle of hydraulic solutal simulation on model was adopted so as to work at a reduced scale. In this case, the phenomena of natural thermal convection in air will be simulated by phenomena of solutal convection in water.

Strict similarity of two experiments involving natural convection should require:

- similarity of geometry;
- identity of the thermal and dynamic adimensional boundary conditions;
- equality of the Stanton numbers

$$(S_t = \frac{Nu}{Ra^{1/2}\,Pr^{1/2}}),$$

which appear in the dimensionless equation of the natural convection.

The equality of Stanton numbers involves identical Rayleigh and Prandtl numbers for the two experiments. Consequently, the Nusselt numbers characterising the two experiments must be equal. Compliance with the Reynolds numbers for the flows generated should also be ensured. This condition is, however, impossible to realise on a reduced-scale model, so that a partial similarity will have to be realised, which will undergo experimental validation.

The solutal simulation of a natural convection phenomenon involves injecting into a reference fluid of density ρ_0, with an insignificant momentum, a fluid of density ρ slightly less than that of the reference fluid. The density difference is obtained by adding to the reference fluid a mass concentration C of a light fluid (ethanol in the case in question). For small density differences $\Delta\rho$ and within the framework of the Boussinesq approximation, it is possible to write $\Delta\rho = \rho - \rho_0 = \beta_m \rho_0 C$. The geometry adopted is a circular plate of diameter D_s, horizontal and heating on the top.

The solutal Rayleigh number is then defined by

$$Ra_m = g\frac{1}{av}\left(\frac{\Delta\rho}{\rho_f}\right)D_s^2, \tag{1}$$

where D_s is the diameter of the source in the model; a represents the molecular diffusivity of the light fluid in the reference fluid, i.e., of ethanol in water; v is the kinematic viscosity of the water–ethanol mixture. All the physical properties of the fluid are taken at the mean value $\rho_f = (\rho + \rho_0)/2$.

For the geometry adopted, the Nusselt number is expressed simply as a function of the Rayleigh number by the correlation [17]:

$$Nu = 0.14\,Ra^{1/3} \quad \text{for } 2\times 10^7 < Ra < 3\times 10^{10}. \tag{2}$$

Similarity conditions require equality of the solutal and thermal Rayleigh numbers ($Ra = Ra_m$), making it possible to determine the density difference $\Delta\rho$ to be imparted to the injection:

$$\frac{\Delta\rho}{\rho_f} = \frac{1}{g}\,Ra\frac{va}{D_s^3}. \tag{3}$$

The Sherwood number Sh, characteristic of the mass transfer to the source, equal to the Nusselt number, can be determined by means of Eq. (2). The mass exchange coefficient h_m at the source level is then given by

$$h_m = \frac{a\,Sh}{D_s}. \tag{4}$$

A flow of lighter mass Φ_m will therefore have to be injected at the source level, corresponding to

$$\Phi_m = h_m S\,\Delta\rho = h_m\frac{\pi D_s^2}{4}\Delta\rho. \tag{5}$$

The light fluid flow to be injected will therefore be

$$Q_s = \frac{\Phi_m}{\Delta\rho}. \tag{6}$$

To ensure satisfactory similarity, one must also have equal or similar Prandtl numbers for the two similar experiments, i.e., equal Schmidt and Prandtl numbers. The latter condition cannot be realised, since the Prandtl number in air is approximately 0.7 whereas the Schmidt number is approximately 1000. However, in a thermal plume in air, the transition to turbulence takes place very rapidly, leading to heat diffusion roughly identical to the diffusion of momentum, on the large scales. In this case, the turbulent Schmidt and Prandtl numbers will be in the vicinity of 1 in both flow configurations, which does not contradict the similarity conditions.

The experimental conditions adopted for a thermal source of diameter $D = 2$ m, with a temperature difference of 65 K relative to the room temperature, lead to a Rayleigh number $Ra = 3.5 \times 10^5$, corresponding to a convected thermal power of approximately $P = 1300$ W. The height of transition to turbulence z_{tr} can be determined when the Rayleigh number based on convective power P reaches the critical value of 10^{10} [18]:

$$Ra = 10^{10} = \frac{g\beta P z_{tr}^2}{D_t \nu k}. \quad (7)$$

This calculation leads to a transition height $z_{tr} = 1.7$ cm and therefore ensures the very rapid establishment of a turbulent flow.

The scale is set at 1/30, thus allowing definition of the various parameters of the hydraulic simulation, given in Table 1. Realistic boundary conditions can be simulated by a periodic distribution of sources in the enclosure, each source being placed at the centre of a square elementary mesh, defined by its side L_m representing the distance separating two sources. The central source surrounded by four sources is thus studied, making it possible to account for the periodicity of boundary conditions on the one hand and to overcome the influence of boundary conditions at the walls of the enclosure on the other hand, to the extent that the sources do not interact with one another.

Table 1
Solutal simulation parameters

D_s (m)	ρ_0 (kg m^{-3})	ρ (kg m^{-3})	ρ_f (kg m^{-3})	$\Delta\rho$ (kg m^{-3})	D_m (m^2 s^{-1})	ν (m^2 s^{-1})	Q_s (ml min^{-1})	Sh	Ra
0.075	998.2	985.1	991.7	13.13	1.13×10^{-9}	1.39×10^{-6}	1.9	457	3.5×10^{10}

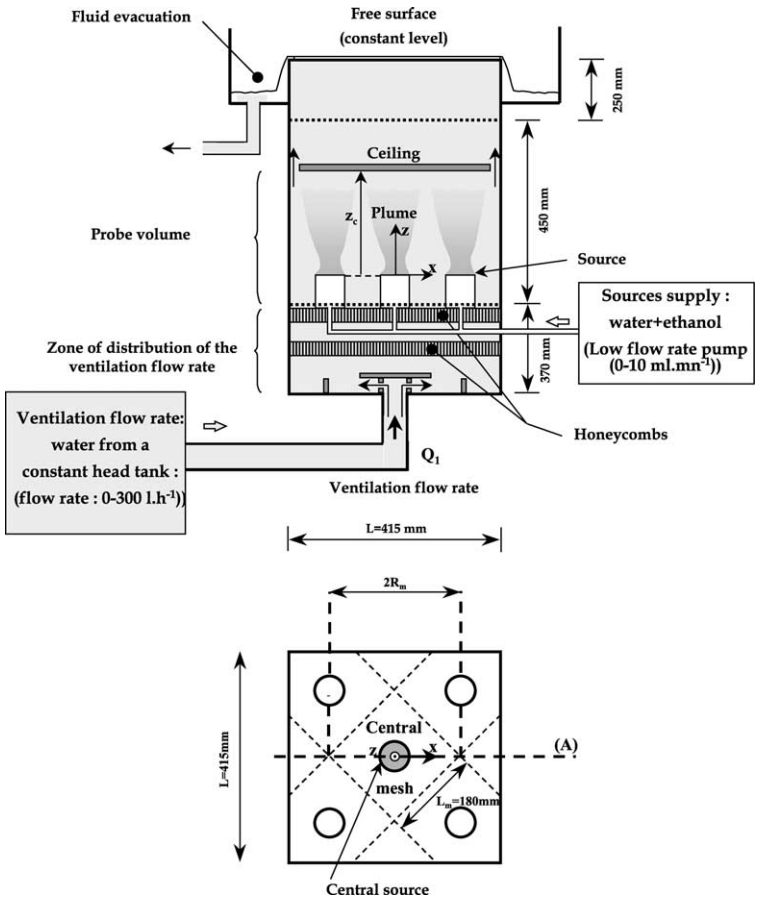

Fig. 2. Experimental set-up.

3. Experimental apparatus

The experiments are performed in a square-base tank of side length $L = 415$ mm (Fig. 2) in which five sources (diameter 75 mm) supplied with light fluid are arranged periodically. The tank is sized so that its area corresponds to the surface area of five whole meshes: the mesh size is therefore $L_m = L \times (5)^{-1/2} = 185$ mm. A small ventilation flow is introduced into the lower part of the tank. It is monitored constantly by an electromagnetic flowmeter. Two consecutive honeycomb structures enable a thoroughly uniform flow to be obtained over the entire basic surface area. The walls were equipped with transparent optical windows so as to visualise the flow and apply optical measurement techniques. The fluid is removed at the ceiling level through slots made in the ceiling. At the top of the tank, fluid is removed so as to maintain a constant hydrostatic pressure throughout the experiment.

A circuit operating by means of a low-delivery pump enables the five sources to be supplied with the same flow rate of a water–ethanol mixture. For each source, the injection region is a disc of porous material, realising a uniform horizontal exchange surface.

4. Measurement techniques

Given the need to disturb the flow as little as possible, non-intrusive optical methods were employed. Laser Doppler velocimetry made it possible to characterise the dynamic field of the plume generated by the source. The velocimeter used consists of an ionised argon laser source, a beam and colour separation module and a Bragg cell. The optical module is equipped with a beam-expander system, to reduce the measurement volume, and a convergent lens of focal length 310 mm. The resulting dimensions of the measurement volume are $(387 \times 47 \times 47\ \mu m^3)$. Contamination of the enclosure by the light fluid and the stratification phenomenon were characterised by a PLIF technique. A fluorescent tracer is diluted to a very small concentration (2 mg l^{-1}) in the light fluid injected at the source level. The fluorescent tracer selected is an organic dye, rhodamine B, used extensively in laser-induced fluorescence [19,20]. The Schmidt number characterising the diffusion of rhodamine B in water is approximately 2700 [21], enabling one to assert that transport of the fluorescent tracer is ensured mainly by the convective and turbulent motions of the flow. The local concentration of the fluorescent tracer is thus equivalent to the local mass fraction of light fluid in the flow.

The general principle of PLIF has already been described by various authors [22] and applied to various flow situations such as jets [23]. It involves exciting the flow by means of a laser sheet and collecting the fluorescence on the matrix of a CCD camera. The main specific difficulty in this experiment is the presence of large optical paths, contributing to attenuation of the incident laser intensity by Beer absorption. The intensity of fluorescence, collected at each point on the CCD sensor corresponding to a flow coordinate point (x,z), depends on the local concentration of the tracer and the local excitation intensity $I(x,z)$ in the form [20]

$$S_f(x,z) = K_{opt}\Phi C(x,z) I_0(x,z)\varepsilon_1 I(x,z), \tag{8}$$

where K_{opt} is a constant characterising the optical chain, Φ the fluorescence quantum efficiency which is constant for constant temperature, $C(x,z)$ the local molecular concentration of the fluorescent tracer and ε_1 the coefficient of absorption of laser radiation in the environment.

The local laser intensity term

$$I(x,z) = I_0(x,z)\ \exp\left[-\int_0^x \varepsilon_1 C(x,z)\,\mathrm{d}x\right]$$

takes into account the space distribution of energy in the laser beam and the Beer attenuation of the incident intensity in the ambient environment [20]. Fluorescence reabsorption phenomena are neglected in this study.

The Beer attenuation term is discretised along x for a given vertical position z (Fig. 3):

$$\exp\left(-\varepsilon_1 \int_0^x C(x,z)\,\mathrm{d}x\right) = \exp\left(-\varepsilon_1 \sum_{i=1}^{n-1} C(x_i)s\right)$$
$$\text{with } x_i = is \text{ and } s = x/n. \tag{9}$$

The fluorescence signal corresponding to the nth pixel of the line located in position z is then

$$\mathrm{CCD}(x_n,z) = K(x_n,z)C(x_n,z)\prod_{i=1}^{n-1}\exp(-\varepsilon_1 C(x_i,z)s), \tag{10}$$

where $K(x_n,z) = K_{opt}\Phi\varepsilon_1 I_0(x_n,z)$.

CCD designates the luminous flux converted into grey levels of a CCD element of the camera's sensible

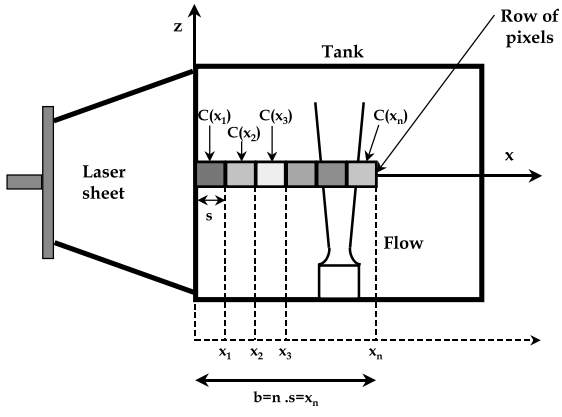

Fig. 3. Local tracer concentration determination principle by planar laser-induced fluorescence (PLIF).

matrix. A preliminary determination of the $K(x_n, z)$ factor is performed by means of a reference image. This factor takes into account the space distribution of energy in the laser beam. For this purpose, a uniform concentration C_0 is established in the tank and an image is produced keeping the same optical alignments and the same optronic parameters. The signal measured on each CCD element is then

$$\mathrm{CCD}_0(x_n, z) = K(x_n, z) C_0 \ \exp(-x_n C_0 \varepsilon_1). \tag{11}$$

It is therefore possible to determine the $K(x_n, z)$ factor.

Relations (10) and (11) enable the concentration at any point $C(x_n, z)$ to be determined as a function of the concentrations determined for the preceding pixels on the same line:

$$C(x_n, z) = \frac{\mathrm{CCD}(x_n, z)}{(\mathrm{CCD}_0(x_n, z)/C_0)\, \mathrm{e}^{x_n C_0 \varepsilon_1}} \prod_{i=1}^{n-1} \mathrm{e}^{\varepsilon_1 C(x_i) s}. \tag{12}$$

The concentration corresponding to each pixel can be determined by successive iterations on a line, neglecting the attenuation on the first pixel.

5. Experimental results

5.1. Plume in infinite environment

The conditions of injection of the light fluid into the source were determined solely on the basis of the equality of the Rayleigh number relative to that of a given heat source. It is therefore essential to verify experimentally the similarity between the behaviour of the flow generated in these circumstances and that of the similar heat source. A series of measurements was thus performed to study the plume created by the central source alone in the model completely filled with water, without a ceiling and without ventilation flow. The measurements were taken in a configuration similar to that of a plume in an infinite environment.

5.1.1. Buoyancy field

To ensure the statistical stability of the mean value measured, 600 images of the field of concentration of the fluorescent tracer are acquired at a frequency of approximately 0.5 Hz, the time for acquisition of an image being equal to (1/25)th s (Fig. 4). The mean concentration radial profiles deduced from this field are of Gaussian shape and can be approximated by

$$C(r, z) = C_\mathrm{c}(z) \ \exp\left(-(r/b_\mathrm{c}(z))^2\right), \tag{13}$$

where $C_\mathrm{c}(z)$ designates the concentration at the centre of the profile, and b_c the characteristic radius such that

$$C(b_\mathrm{c}, z) = \frac{C_\mathrm{c}(z)}{\mathrm{e}}. \tag{14}$$

The evolution of this concentration radius as a function of the height is shown in Fig. 5. The minimum radius

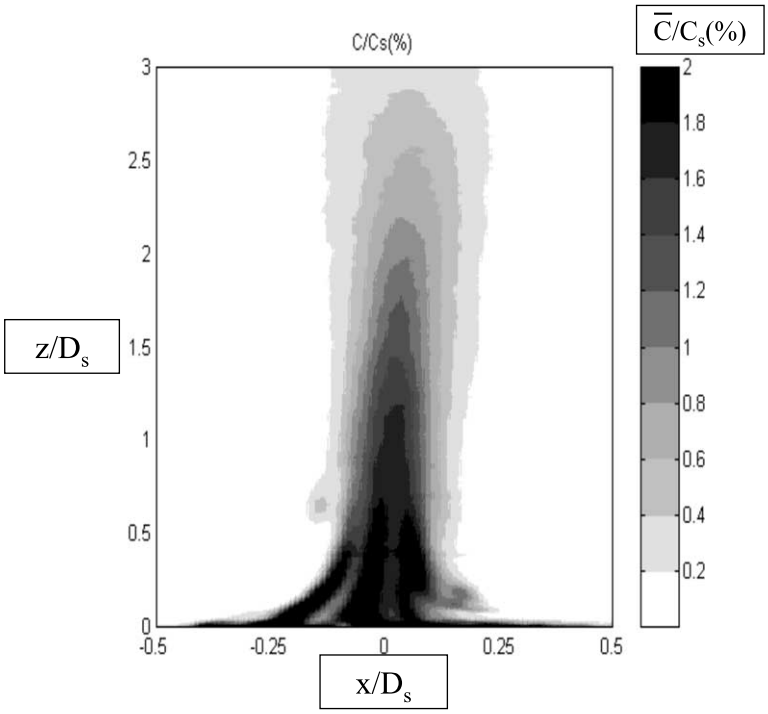

Fig. 4. Laser-induced fluorescence image of the concentration field in the solutal plume ($D_\mathrm{s} = 0.075$ m; $B_\mathrm{s} = 4.22 \times 10^{-9}$ m^4 s^{-3}).

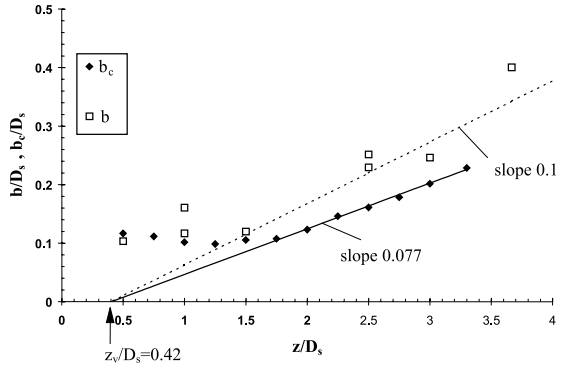

Fig. 5. Evolution of dynamic and buoyancy radius as a function of the elevation above the ($D_s = 0.075$ m; $B_s = 4.22 \times 10^{-9}$ m^4 s^{-3}.)

value is attained at a distance of approximately $z/D_s = 1.2$ above the source, corresponding to maximum contraction of the plume. Beyond a distance $z/D_s = 1.75$, the evolution of the concentration radius with height is linear [10] and enables the position of a virtual origin z_v to be determined at distance $z_v/D_s = 0.42$. The plume's expansion is then characterised by

$$b_c = 0.077(z - z_v). \tag{15}$$

The radial concentration profiles shown in Fig. 6 are reduced to the form

$$\frac{C(r,z)}{C_c(z)} = \exp\left(-p(r/(z-z_v))^2\right). \tag{16}$$

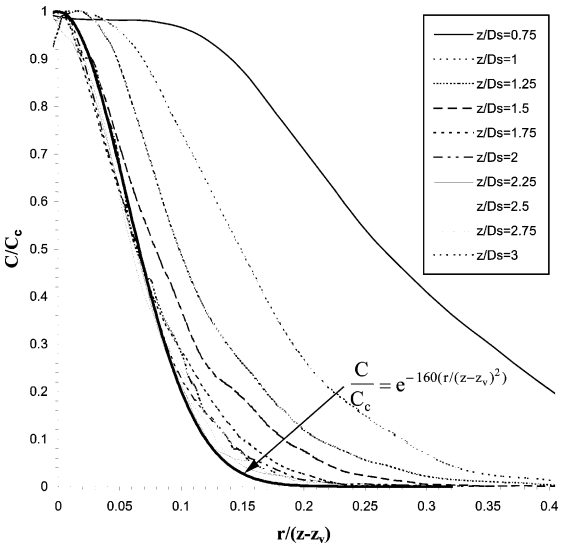

Fig. 6. Radial profiles of the normalized concentration for different elevation above the source ($D_s = 0.075$ m; $B_s = 4.22 \times 10^{-9}$ m^4 s^{-3}).

The affinity of the reduced profiles is clearly verified from $z/D_s = 1.75$ and a value of $p = 160$ can be determined.

5.1.2. Velocity field

Speed profiles were measured at various heights above the source. This type of natural convection flow shows strong fluctuations at low frequency and low speed. The signals were sampled at a frequency of approximately 50 Hz. The acquisition time, selected so as to ensure statistical stability of the mean value of the vertical component of velocity, ranges between 6 and 10 min.

The radial profiles corresponding to the vertical component of velocity are of Gaussian shape. They can be adjusted by an expression of the type

$$w(r,z) = w_c(z)\ \exp\left(-(r/b(z))^2\right), \tag{17}$$

where w_c is the vertical component of velocity on the central axis of the profile and $b(z)$ the dynamic radius defined by

$$w(b,z) = \frac{w_c(z)}{e}. \tag{18}$$

The evolution of the dynamic radius $b(z)$ as a function of height z above the source is also shown in Fig. 5. Despite the scatter of results, it is possible to roughly distinguish between two flow regions. The first corresponds to the region of plume development for $z/D_s < 1.7$, and the second to the developed region where $b(z)$ increases almost linearly with height. The linear evolution of b makes it possible, in the same way as for the concentration profiles, to locate the virtual origin z_v such that

$$b = 0.1(z - z_v) \quad (\text{with } z_v/D_s = 0.42). \tag{19}$$

The radial profiles of the vertical component of velocity can be reduced to the form

$$\frac{w(r,z)}{w_c(z)} = \exp\left(-m(r/(z-z_v))^2\right). \tag{20}$$

The grouping of the normalized measured profiles (Fig. 7) seems correct from $z/D_s = 1.5$ and a value of $m = 95$ seems satisfactory.

The flow entrained by the plume at height z can be determined by integration of the radial profile of velocity (Eq. (17)):

$$Q(z) = 2\pi \int_0^\infty w(r,z) r\, dr = \pi w_c(z) b^2. \tag{21}$$

Thus, by estimating flow rates, it is possible, for heights greater than $z/D_s = 1.7$, to formulate a law of the type

$$z - z_v = 3.3 B_s^{-1/5} Q^{3/5} \tag{22}$$

which is in full agreement with the law of the flow entrained by a fully developed plume flow [6].

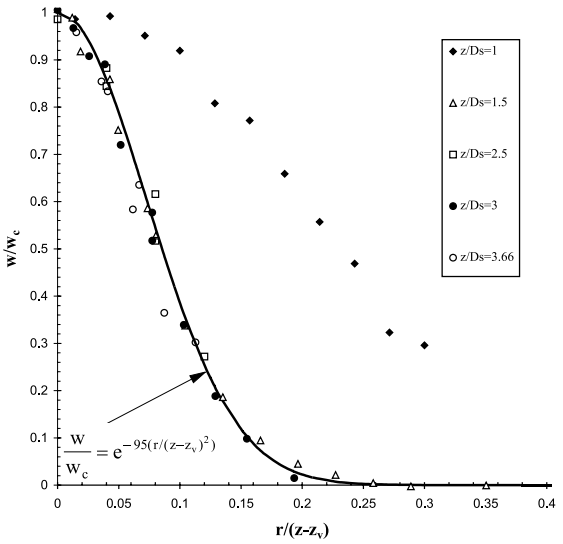

Fig. 7. Radial profiles of the normalized vertical component of the velocity for different elevation above the source ($D_s = 0.075$ m; $B_s = 4.22 \times 10^{-9}$ m^4 s^{-3}).

5.1.3. Description of the plume

The plume model proposed by Morton et al. [24], based on the assumption of self-similarity, allows the fully developed plume flow to be described. Like the authors cited, we shall designate by α and λ the coefficient of entrainment and the ratio between the buoyancy radius and the dynamic radius. The expressions resulting from this model giving the dynamic radius b, the vertical component of velocity W and the entrained flow Q as a function of height relative to the virtual origin of the plume, are given by

$$b = \frac{6\alpha}{5}(z - z_v), \tag{23}$$

$$w_c = \left(\frac{3(\lambda^2+1)}{2\pi}\right)^{1/3}\left(\frac{5}{6\alpha}\right)^{2/3} B_s^{1/3}(z - z_v)^{-1/3}, \tag{24}$$

$$Q = \pi\left(3\frac{(\lambda^2+1)}{2\pi}\right)^{1/3}\left(\frac{6\alpha}{5}\right)^{4/3} B_s^{1/3}(z - z_v)^{5/3}. \tag{25}$$

The value of entrainment coefficient α can be determined from relations (19) and (25):

$$b = \frac{6\alpha}{5}(z - z_v) = 0.1(z - z_v) \quad \text{or} \quad \alpha \cong 0.085. \tag{26}$$

It can also be found by adjusting the radial profiles of velocity (Eq. (20)):

$$\alpha = (5/6)m^{-1/2} = 0.085. \tag{27}$$

Ratio λ, which is the ratio between the characteristic buoyancy radius represented by the rhodamine B concentration and the dynamic radius, can be determined by

$$\lambda \cong \frac{b_c}{b} = \left(\frac{m}{p}\right)^{1/2} = \left(\frac{95}{160}\right)^{1/2} = 0.77. \tag{28}$$

The values assigned to parameters α and λ based on our measurements are consistent with the values available in the literature and determined for plumes generated by various types of buoyancy sources [4,25,26], and especially for thermal plumes in air [3,27].

The measurements presented enable us to show that the plume generated in the simulation tank can be described by laws similar to those for the thermal plume in air. We are therefore able to simulate a source of natural convection in a confined stratified enclosure. This study can therefore contribute to characterisation of the parameters governing this stratification.

5.2. Plume in confined stratified environment

The experimental results concerning the plume configuration in a confined environment are examined here. Only the flow in the central mesh of the model is considered.

An endeavour was made to formulate a law describing the evolution of the stratification height in the enclosure. Various cases defining the buoyancy source by its diameter D_s and its buoyancy flux B_s were studied:

- $B_s = B_{s1} = 4.22 \times 10^{-9}$ m^4 s^{-3} with $D_s = D_{s1} = 0.075$ m;
- $B_s = B_{s2} = 2.55 \times 10^{-8}$ m^4 s^{-3} with $D_s = D_{s1} = 0.075$ m;
- $B_s = B_{s2} = 2.55 \times 10^{-8}$ m^4 s^{-3} with $D_s = D_{s2} = 0.045$ m.

Various ceiling heights were also considered in each case.

The flow in the enclosure subject to a ventilation flow rate Q_1 is characterised by a vertical density stratification. This stratification stabilises after a certain settling time following the simultaneous start-up of the buoyancy sources and the ventilation flow. This steady-state condition is achieved especially rapidly with high ventilation flow rates. It can be observed that the shape of the vertical concentration profiles is stabilised after a time corresponding to between 5 and 10 tank renewals.

5.2.1. Characterisation of the interface

The definition of the interface elevation has been dealt with by certain authors. Mierzwinski et al. [13] proposed definitions based on the shape of the mean temperature or concentration profiles. We propose here defining an interface elevation and thickness based on statistical processing performed on fluctuations of the concentration field. When the flow's steady-state regime

is achieved, a series of approximately 1000 images distributed over 500 s is produced. Using the decomposition into mean and fluctuating values $C = \bar{C} + c$, it is possible to calculate, from this series of images, the mean value $\bar{C}$ and the standard deviation σ of the concentration fluctuations. For a sufficiently large number of images, the skewness factor S and flatness factor F can be estimated.

Thus, outside of the central region corresponding to the plume, it is possible to obtain vertical profiles of the various statistical moments, so as to characterise the vertical stratification in the enclosure. Analysis of the mean concentration field (Fig. 8) shows two regions in the enclosure: a lower region in which the concentrations are very less, and an upper region in which they appear much greater. Fig. 9 shows the evolution of the vertical profiles for various ventilation flow rates. These profiles make it possible, first, to visualise the increase in the stratification level as the ventilation flow rate increases. For low flow rates where the stratification elevation is close to the source level (e.g., $Q_1 = 25\ \mathrm{l\ h^{-1}}$), these profiles indicate the presence of two very uniform regions separated by a fine interface. For higher flow rates (e.g., $Q_1 = 245\ \mathrm{l\ h^{-1}}$), the interface becomes thicker and a vertical concentration gradient is visible in the upper flow region. It then becomes harder to define the position of the interface without employing another quantity. Thus, it seems possible to locate this position z_i precisely as the position of the maximum standard deviation of the concentration fluctuations (Fig. 10). This definition corresponds to a physical criterion, since the interface region can be compared to a region in which two fluids of different buoyancy mix. The standard deviation of the concentration fluctuations, corresponding to that for density fluctuations, is one of the characteristics of mixing. The skewness and flatness factors are equal to 0 and 3, respectively, outside of the regions defining the interface, corresponding to a Gaussian distribution of concentration fluctuations. Two extrema can be noted on the vertical profile of the skewness coefficient. The distance δ separating these two extrema makes it possible to give a criterion representative of the thickness of the region of mixing of the two fluids of different buoyancy, defining the interface. The antisymmetric aspect of the asymmetry factor shows that the mean concentration is as much the result of concentrations greater than the mean as of concentrations lower then the mean. The positions of the maximum flatness factor values confirm the data supplied by the skewness coefficient.

Some interface thicknesses determined with the previous definition are shown in Fig. 11. A regular increase in the interface thickness with stratification height is observed. In both the cases presented, corre-

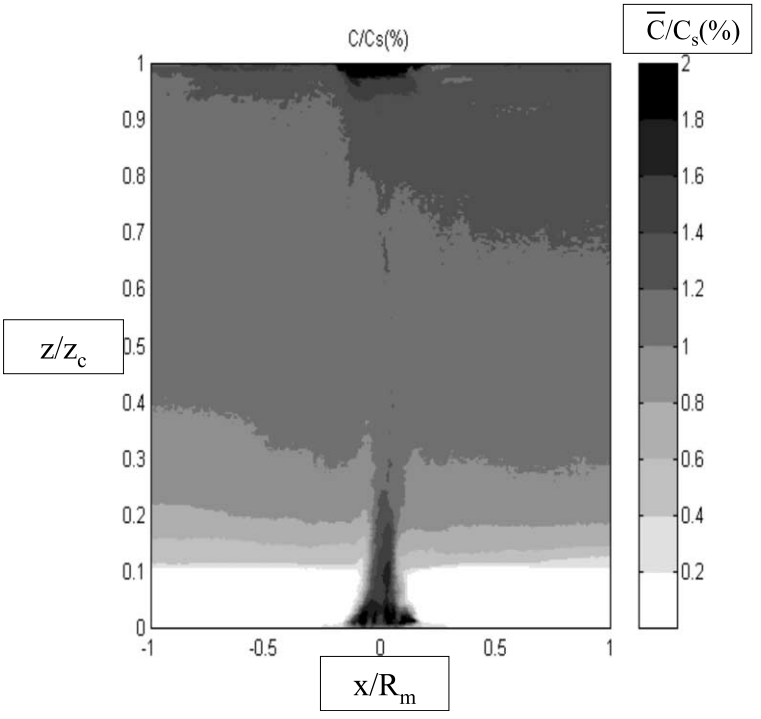

Fig. 8. Laser-induced fluorescence image of the concentration field in the stratified and confined enclosure ($D_s = 0.045$ m; $B_s = 2.55 \times 10^{-9}\ \mathrm{m^4\ s^{-3}}$, $Q_1 = 90\ \mathrm{l\ h^{-1}}$, $z_c = 0.15$ m).

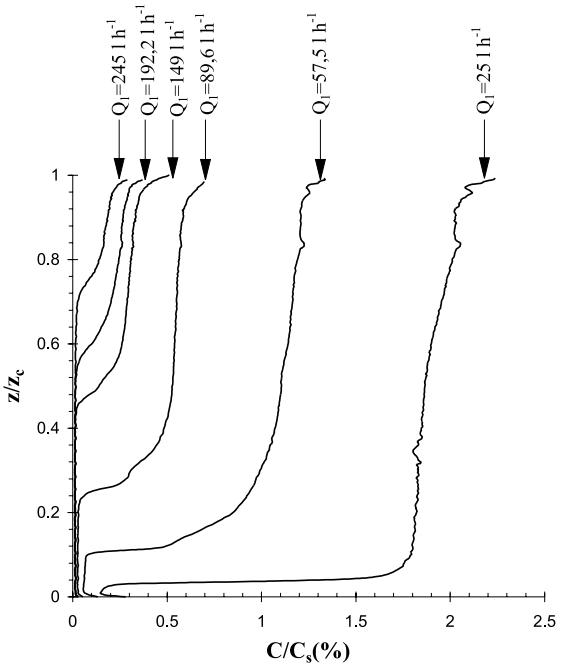

Fig. 9. Vertical distribution of the mean concentration measured at $x/R_m = 0.5$ for different ventilation flow rate ($D_s = 0.045$ m; $B_s = 2.55 \times 10^{-9}$ m^4 s^{-3}, $z_c = 0.15$ m).

sponding to different buoyancy fluxes at the source, it appears that the thicknesses are of the same order of magnitude. The region of plume development is characterised by a regular increase in the dynamic turbulence intensity on the axis of the plume [10]. The increase in interface thickness with elevation above the source is probably related to the intensity of the turbulent fluctuations at the elevation at which the interface is formed.

5.2.2. Study of stratification height

The stratification height having been defined clearly, it is now possible to formally process the experimental results. The influence of parameters such as the ceiling height and the method of exhausting fluid through the ceiling has not been able to be illustrated significantly. Only the effects of the ventilation flow rate Q_1, the source diameter D_s and the buoyancy flux at source B_s will therefore be considered.

5.2.2.1. Developed plume region. The evolution of the stratification height is usually established based on the formulation of the entrained flow, for stratification heights measured at sufficiently large distances above the source (developed region of a plume). The law describing the entrained flow for a steady-state plume is written in the form [6]

$$Q \propto B_s^{1/3}(z - z_v)^{5/3}, \tag{29}$$

where $z - z_v$ is the distance from the virtual origin of the plume.

Based on this result, a proportional relationship between the stratification height in the enclosure and quantity $Q_1^{3/5}B_s^{-1/5}$ can be observed [12,28]. Fig. 12 shows that the stratification heights measured at distances greater than 0.5 source diameter above the source are correctly described, for a flow rate corresponding to 5 plumes, by [1]

$$z_i - z_v = 1.68B_s^{-1/5}Q_1^{3/5} \quad (z_i > 0.5D_s). \tag{30}$$

This result therefore confirms the data available for the steady-state plume region. On the other hand, no result is available in the literature for the region close to the source ($z < 0.5Ds$).

5.2.2.2. Region close to the source. Fig. 12 shows that the previous formulation is no longer suitable for stratification heights measured closer to the source. In the close region ($z < 0.5D_s$), two parameters, the ventilation flow rate and the buoyancy flux at source, are no longer sufficient to describe the evolution of the stratification height. The source geometry and especially its diameter must influence the stratification height. It has been found that, at a given ventilation flow rate, the stratification height was increased sharply (by approximately 35%) when this parameter was reduced by 40%, i.e., by going from $D_s1 = 0.075$ m to $D_{s2} = 0.045$ m. Simple dimensional considerations enable the interface elevation z_i to be formulated by a relation of the type

$$z_i \propto \left(Q_1^3 B_s^{-1}\right)^n D_s^{1-5n}. \tag{31}$$

Adopting the value $n = 1/2$, Fig. 13 shows that the preceding formulation gives a good description of the height in the three cases considered experimentally for z_i heights of less than 0.6 source diameter. This leads to the following proposition for stratification in the vicinity of the source for a flow rate corresponding to 5 plumes: [2]

$$z_i \cong 0.56Q_1^{3/2}B_s^{-1/2}D_s^{-3/2} \quad (z_i < 0.6D_s). \tag{32}$$

Beyond 0.6 source diameter, it has been shown that the evolution of the stratification heights was correctly described by a $Q_1^{3/5}B_s^{-1/5}$ law.

[1] Eq. (30) is written for 5 plumes in the enclosure. If there is only 1 plume, the relation $z_i - z_v = 4.41B_s^{-1/5}Q_l^{3/5}$ should be used.

[2] Eq. (32) is written for 5 plumes in the enclosure. If there is only 1 plume, the relation $z_i = 6.26Q_l^{3/2}B_s^{-1/2}D_s^{-3/2}$ should be used.

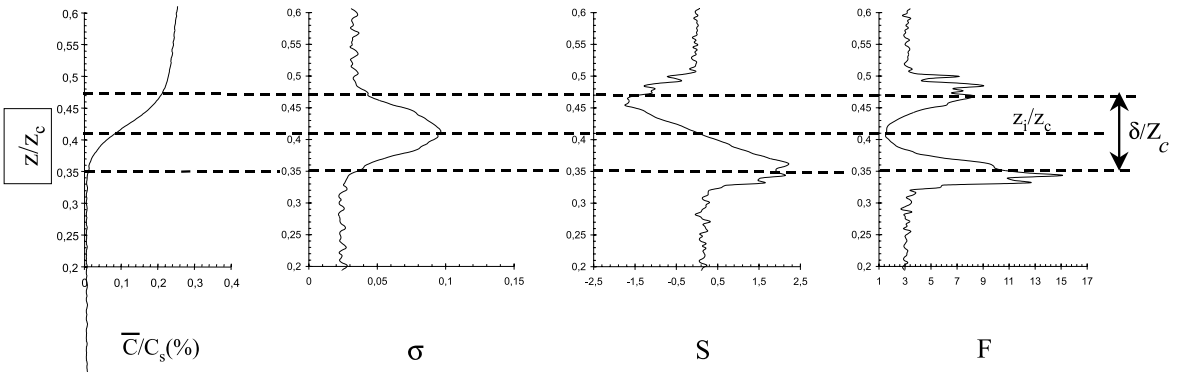

Fig. 10. Vertical distribution of mean concentration, root mean square, skewness factor and flatness factor of the concentration fluctuations, measured at $x/R_m = 0.5$ ($D_s = 0.075$ m; $B_s = 4.22 \times 10^{-9}$ m^4 s^{-3}, $Q_l = 90$ l h^{-1}).

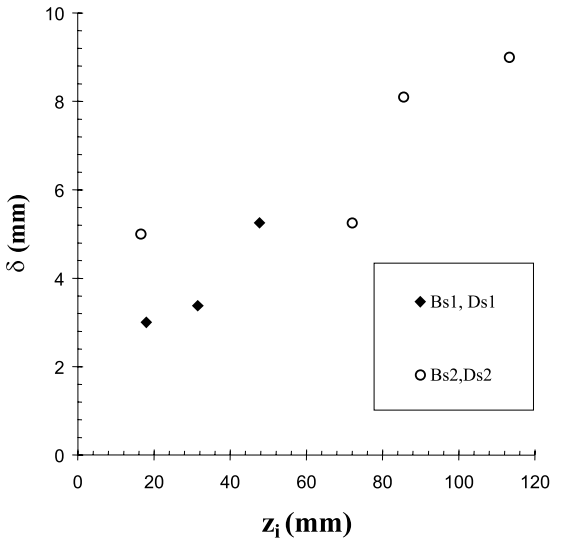

Fig. 11. Evolution of the measured interface thickness δ as a function of the interface elevation.

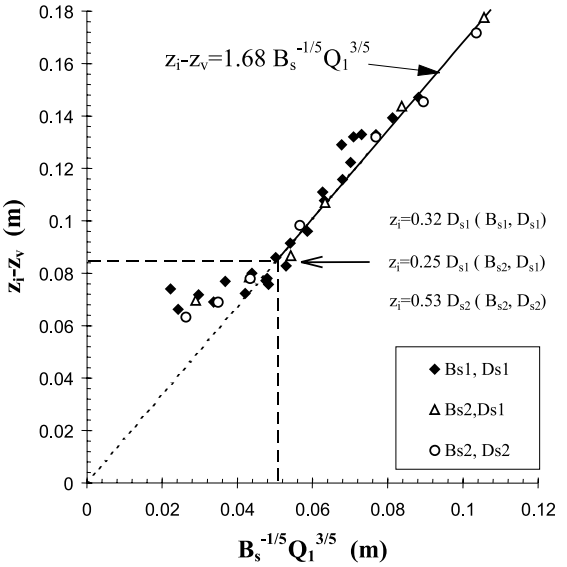

Fig. 12. Evolution law of the interface elevation.

5.2.3. Relationship between the two regions

It now seems worthwhile verifying the good relationship between the stratification height laws proposed for the two flow regions. It seems appropriate here to present these laws in dimensionless form. For the developed plume region, relation (31) can be expressed as a function of the quantities involved in the similarity [29]

$$\left(\frac{z_i - z_v}{D_s}\right)^{5/3} = KX, \tag{33}$$

where K is a constant and

$$X = \frac{Q_l}{D_s \upsilon}\left[\frac{Sc^2}{Ra_m^{4/3}}\right]^{1/3}$$

a dimensionless number established using an expression of the Nusselt number of the $Nu \propto Ra^{1/3}$ type.

In the same way, the evolution of the stratification height in the region close to the source (Eq. (32)) can be expressed in the following form:

$$\left(\frac{z_i}{D_s}\right)^{2/3} = K'X, \tag{34}$$

where K' is a constant.

Thus, in the two regions in question, the quantities $(z_i - z_v/D_s)^{5/3}$ and $(z_i/D_s)^{2/3}$ can be expressed as a function of the same dimensionless variable X. This variable was estimated for each experiment considering the physical properties of the fluids at their film value. The heights measured seem suitably grouped by this type of non-dimensioning. By adjusting the measurements for the two flow regions, it can be shown that the

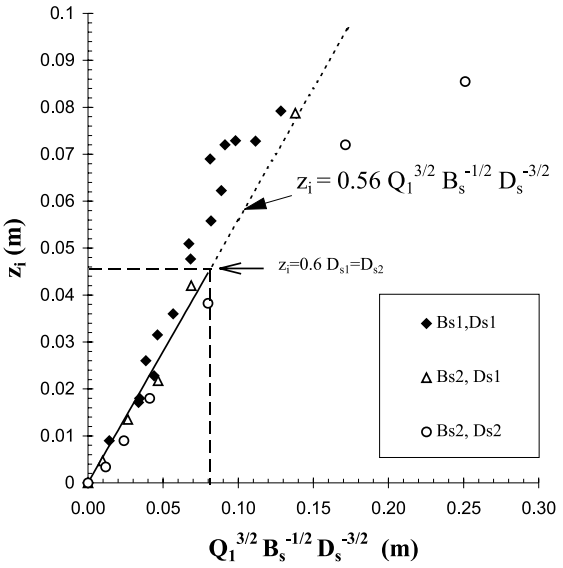

Fig. 13. Evolution law of the interface elevation.

interface point for the two laws is located around value $X = 0.7$ (Figs. 14(a) and (b)). The two laws obtained, corresponding to the two flow regions, can be written as [3]

$$\left(\frac{z_i - z_v}{D_s}\right)^{5/3} \cong 3.85X \quad \text{for } X > 0.7, \tag{35}$$

$$\left(\frac{z_i}{D_s}\right)^{2/3} \cong 1.1X \quad \text{for } X < 0.7. \tag{36}$$

6. Conclusions

A solutal simulation of a thermal plume in a confined environment was performed based on equality of the thermal and solutal Rayleigh numbers. The addition of an auxiliary ventilation flow made it possible to create stratification conditions in the enclosure, so as to simulate a displacement ventilation installation.

The injection of a fluorescent tracer at the level of the buoyancy source made it possible to characterise the density stratification by visualising the tracer concentration field through the planar laser-induced fluorescence (PLIF) technique. Criteria permitting definition of the interface elevation and thickness, respectively, were determined based on statistical processing of concentration fluctuations.

Based on these criteria, the assumptions commonly used in the literature to describe the stratification height as a function of buoyancy and ventilation flow rate were verified in the fully developed plume region. These results were extended to the region close to the source, where it was necessary to employ, in particular, the characteristic source dimension in the formulation of this height.

In numerous real conditions, the ceiling height is of the order of magnitude of the characteristic source dimension, which shows that the established laws should make it possible to make a major contribution to the design of displacement ventilation installations.

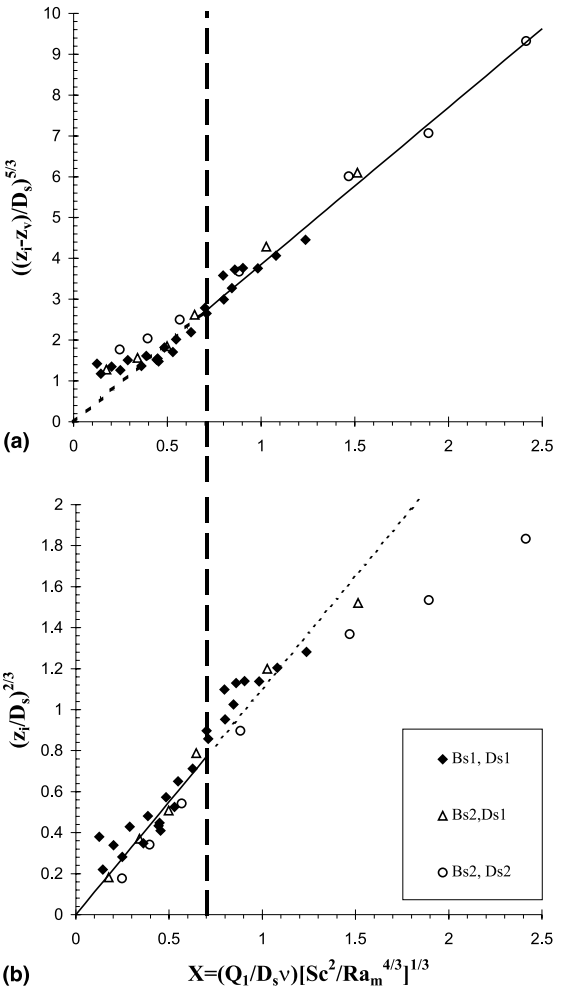

Fig. 14. Non-dimensional presentation of the evolution law of the interface elevation: (a) in the fully developed plume zone; (b) in the vicinity of the source.

References

[1] M. Sandberg, S. Lindström, A model for ventilation by displacement, in: RoomVent'87, 1987.

[3] Eqs. (35) and (36) are written for 5 plumes in the enclosure. If there is only 1 plume, the coefficient in front of the variable X should be multiplied by 5.

[2] J.S. Turner, Buoyancy Effects in Fluids, Cambridge University Press, Cambridge, London, 1972.
[3] H. Nakagome, M. Hirata, The Structure of Turbulent Diffusion in an Axisymmetrical Plume, ICHMT, Dubrovnik, 1976.
[4] P.N. Papanicolaou, E.J. List, Investigations of round vertical turbulent buoyant jets, J. Fluid Mech. 195 (1988) 341–391.
[5] Z. Dai, L.K. Tseng, G.M. Faeth, Structure of round, fully developed buoyant turbulent plumes, ASME J. Heat Transfer 116 (1994) 409–417.
[6] G.K. Batchelor, Heat convection and buoyancy effects in fluids, Quart. J. Roy. Met. Soc. 80 (1954) 339–358.
[7] B.R. Morton, The choice of conservation equations for plume models, J. Geophys. Res. 76 (1971) 7409–7416.
[8] P. Kofoed, Thermal plumes in ventilated rooms, Ph.D. Thesis, Aalborg University, Denmark, 1991.
[9] I. Welling, H. Koskela, T. Hautalampi, Experimental study of the natural-convection plume from a heated vertical cylinder, Exp. Heat Transfer 11 (1998) 135–149.
[10] B. Guillou, M. Brahmini, Doan–Kim–Son Structure turbulente d'un panache thermique. Aspect dynamique, J. Méc. Theor. Appl. 5 (1986) 371–401.
[11] Z. Popiolek, S. Mierzwinski, Buoyant plume calculation by means of the integral method, A4_series No. 89, Department of Heating and Ventilating, Royal Institute of Technology, Stockholm, Sweden, 1984.
[12] M. Sandberg, S. Lindström, Stratified flow in ventilated rooms – a model study, in: RoomVent'90, 1990.
[13] S. Mierzwinski, Z. Popiolek, Z. Trzeciakiewicz, Experiments on two-zone air flow forming in displacement ventilation, in: RoomVent'96, 1996.
[14] S. Pinard, J.-L. Tuhault, D. Blay, Etude expérimentale d'un système de climatisation par déplacement, in: SFT Congress 98, Marseilles, May 5–7, 1998.
[15] D. Manzoni, P. Guitton, Validation of displacement ventilation simplified models, in: Building Simulation'97, vol. 1, 1997, pp. 233–239.
[16] W.D. Baines, A technique for the direct measurement of volume flux of a plume, J. Fluid Mech. 132 (1983) 247–256.
[17] W.H. Mc Adams, Transmission de la chaleur, Dunod (Libraire), Paris, 1962.
[18] A. Bejan, Convection Heat Transfer, Wiley/Interscience, New York, 1984.
[19] M.L. Viriot, J.C. André, Fluorescent dyes: a search for new tracers for hydrology, Analusis 17 (1989) 97–111.
[20] F. Lemoine, M. Wolff, M. Lebouché, Exp. Fluids (1996).
[21] C.R. Reid, J.M. Prausnitz, B.E. Poliny, The Properties of Gases and Liquids, McGraw-Hill, New York, 1986.
[22] P.S. Karano, M.G. Mungal, PLIF measurements in aqueous flows using the Nd:YAG laser, Exp. Fluids 23 (1997) 382–387.
[23] I. Van Cruyningen, A. Lozano, R.K. Hanson, Quantitative imaging of concentration by planar laser-induced fluorescence, Exp. Fluids 9 (1990) 41–49.
[24] B.R. Morton, J. Taylor, J.S. Turner, Turbulent gravitational convection from maintained and instantaneous sources, Proc. Roy. Soc. London, Ser. A 234 (1956) 1–23.
[25] H. Rouse, C.S. Yih, H.W. Humphreys, Gravitational convection from a boundary source, Tellus 4 (1952) 201–210.
[26] W.K. George, R.L. Alpert, F. Tamini, Turbulence measurements in an axisymmetric plume, Int. J. Heat Mass Transfer 20 (1977) 1145–1154.
[27] P. Kofoed, P.V. Nielsen, Thermal plumes in ventilated rooms: measurements in stratified surroundings and analysis by use of an extrapolation method, in: Roomvent'90, 1990.
[28] W.D. Baines, J.S. Turner, Turbulent buoyant convection from a source in a confined region, J. Fluid Mech. 37 (1969) 51–80.
[29] O. Auban, Approche expérimentale de la ventilation par déplacement, Ph.D. Thesis, Henri Poincaré University, Nancy, France, 2000.